Cellulose (2016) 23:2929–2942
DOI 10.1007/s10570-016-1034-7

ORIGINAL PAPER

Biopolyols obtained via crude glycerol-based liquefaction of cellulose: their structural, rheological and thermal characterization

Paulina Kosmela · Aleksander Hejna · Krzysztof Formela · Józef T. Haponiuk · Łukasz Piszczyk

Received: 1 April 2016 / Accepted: 30 July 2016 / Published online: 9 August 2016
© The Author(s) 2016. This article is published with open access at Springerlink.com

Abstract In this work lignocellulose biomass liquefaction was used to produce biopolyols suitable for the manufacturing of rigid polyurethane foams. In order to better evaluate the mechanism of the process, pure cellulose was applied as a raw material. The effect of time and temperature on the effectiveness of liquefaction and the parameters of resulting biopolyols were characterized. The prepared materials were analyzed in terms of their chemical structure, rheology, thermal and oxidative stability, and basic physical and mechanical properties that are important from the point of view of polyurethane manufacturing. The optimal parameters for the biopolyol production with a 94 % yield were achieved at 150 °C for a 6-h reaction duration. The obtained polyols were characterized by the hydroxyl number of 643 mg KOH/g and enhanced thermal and oxidative stability compared to the polyols obtained at lower temperatures, which is associated with the altered mechanism of liquefaction. The results of rheological tests, analyzed with the use of Ostwald-de Waele and Herschel Bulkley models, revealed that the prepared biopolyols can be classified as pseudoplastic fluids with the viscosity values similar to those of commercially available products. Rigid foams obtained via partial substitution of petrochemical polyol with prepared bio-based one were characterized by slightly increased apparent density and average cell size comparing to unmodified materials. The best mechanical performance was observed for the sample containing 35 wt% of biopolyol in the polyol mixture, which indicates a synergistic effect between the applied polyols. The applied modification delayed thermal degradation of foams due to changes in thermal decomposition process. In conclusion, the presented work confirms that lignocellulose biomass liquefaction can be successfully applied as a manufacturing method of polyols later used in the production of polyurethanes.

Keywords Biopolyols · Biomass liquefaction · Crude glycerol · Rigid polyurethane foams

P. Kosmela · A. Hejna · K. Formela · J. T. Haponiuk · Ł. Piszczyk (✉)
Department of Polymer Technology, Faculty of Chemistry, Gdansk University of Technology, G. Narutowicza Str. 11/12, Gdansk, Poland
e-mail: paulina.kosmela@gmail.com

A. Hejna
e-mail: ohejna@wp.pl

K. Formela
e-mail: krzform1@pg.gda.pl

J. T. Haponiuk
e-mail: jozhapon@pg.gda.pl

Ł. Piszczyk
e-mail: lukpiszc@pg.gda.pl

Introduction

Due to high cost and non-renewable character of petroleum as well as inconveniences associated with

the utilization of huge amounts of various by-products, pro-ecological technologies are gaining increasing attention in scientific and industry-related circles. These technologies include the processes related to the utilization of biomass not only at the energy production stage, but also during the fabrication of various chemical compounds. To some extent, such biomass utilization helps to cope with the surplus of biomass stored in landfills.

The main component of biomass is lignocellulose, which is a combination of natural polymers such as cellulose, hemicellulose and lignin, containing at least two hydroxyl groups per particle. Its functionalized structure makes lignocellulose biomass a very desirable substrate for many chemical processes, e.g. liquefaction. The application of the chemical methods of lignocellulose biomass liquefaction results in the synthesis of highly reactive compounds with a vast range of molecular weight, which can be further processed into phenolic resins (Roslan et al. 2014; Wang et al. 2009a, b) or polyols for the production of polyurethanes (Cinelli et al. 2013; Hu et al. 2012; Kurimoto et al. 2001; Wang et al. 2008).

The most popular methods of biomass liquefaction are based on the incorporation of organic solvents and acidic or basic catalysts (Hassan and Shukry 2008). The conversion of biomass, very often wood, into industrially useful compounds can also be performed with the use of supercritical methanol or ethanol (Minami and Saka 2003; Poudel and Oh 2012), subcritical water (Matsunaga et al. 2008) or ionic liquids (Maki-Arvela et al. 2010). The main reactions occurring during liquefaction are the degradation of biomass ingredients, esterification and polycondensation. The final structure of the obtained products mainly depends on the solvent used, and the conditions of the process (Ye et al. 2014).

Oxypropylation with propylene oxide, assisted by Brønsted or Lewis base as a catalyst, is one of the most popular methods of polyol production from lignocellulose biomass. The essence of this method is to enhance the reactivity of hydroxyl groups by shifting them towards the end of the main chain (Briones et al. 2011a, b). The resulting polyols are liquid mixtures of oxypropylenated biomass, homopolymer of propylene oxide, and unreacted biomass (Evtiouguina et al. 2002). This method of polyol production was investigated by many research groups which incorporated into the process various types of biomass such as, coffee grinds (Evtiouguina et al. 2002), sugar beet pulp (Pavier and Gandini 2000), gambier tannin (Arbenz and Averous 2015), soy hulls (Rosa et al. 2015), rapeseed cake residue (Briones et al. 2010), and olive stones (Matos et al. 2010).

Besides propylene oxide, the most popular solvents used for biomass liquefaction are polyethylene glycol (PEG), ethylene glycol (EG) and glycerol. Zhang et al. (2007) used ethylene glycol to liquefy bagasse in the presence of sulfuric acid (VI), while Ye et al. (2014) converted bamboo shoot shells into a polyol with the mixture of EG and PEG. Glycerol, used alone or in combination with other solvents, seems to be the most popular chemical to liquefy cork (Yona et al. 2014), acid hydrolysis residue of corncob (Zhang et al. 2012), biodiesel production solid residues (Briones et al. 2011a, b), wheat straw (Wang and Chen 2007), and bagasse or cotton stalks (Hassan and Shukry 2008). The main advantage of glycerol with respect to the liquefaction process is the presence of three hydroxyl groups in its structure, which allows for the generation of the branched structure of resulting polyols. Recently, the attempts of crude glycerol incorporation into the liquefaction process of corn straw (Hu and Li 2014) and soybean straw (Hu et al. 2012) have been reported.

In order to better understand the mechanism of the process, polyols can also be obtained from the individual biomass compounds such as, cellulose or lignin. Lignin can be converted into polyols via hydrolysis in the presence of basic catalysts (Mahmood et al. 2013), and the treatment with organic solvents (Jin et al. 2011) or supercritical methanol and ethanol (Miller et al. 1999). The methods of cellulose liquefaction are based on cellulose hydrogenolysis or hydrolysis assisted by acids, enzymes, ionic liquids or hot steam (Baek et al. 2012; Liu et al. 2012). Zhang et al. (2014) carried out acid-catalyzed liquefaction of three main components of biomass, i.e. cellulose, hemicellulose and lignin with the mixture of polyethylene glycol and glycerol in order to study in detail the mechanisms of this process. The authors stated that liquefaction of cellulose should be performed at a temperature around 160 °C to achieve the best effectiveness.

In the presented study, the potential use of refined crude glycerol as a solvent for cellulose liquefaction has been evaluated. Based on the literature data, we aimed at examining the influence of the time of

MOST WIEDZY Downloaded from mostwiedzy.pl

reaction (1–6 h) and temperature (120–150 °C) on the yield of the process as well as the chemical structure (FTIR analysis), water content, hydroxyl value, and rheological (viscosity studies) and thermal (thermogravimetric analysis, oxidation onset temperature test) properties of the resulting biopolyols. Pure cellulose was used to better control the liquefaction process with refined crude glycerol. Moreover, a selected biopolyol was applied to prepare rigid polyurethane foams.

Experimental

Materials

Bio-based polyols were synthesized by liquefaction of cellulose with the purified crude glycerol. Cellulose in the form of cotton with a water content of 5.4 % was obtained from VITA Rzeszow (Poland). Refined crude glycerol was acquired from Bio-Chem Sp. z o.o. (Poland). The water content of the solvent was lower than 0.5 wt% and its density was 1.26 g/cm^3. The liquefaction process was catalyzed by 95 % water solution of sulfuric acid (VI) obtained from Avantor Performance Materials Poland SA.

Rigid polyurethane foams were synthesized using two types of polyols, namely, petrochemical polyetherol based on sorbitol with a trade name Rokopol RF55, and previously prepared biopolyol EP1 (see "Preparation of bio-based polyols" section). Rokopol RF55, with a hydroxyl number (L_{OH}) of ca. 495 mg KOH/g and the water content lower than 0.1 wt%, was supplied by PCC Rokita SA (Poland). The applied bio-based polyol was characterized by $L_{OH} = 754$ mg KOH/g and the water content of 0.63 wt%. Polymeric methylene diphenyldiisocyanate (pMDI) was supplied by Borsodchem (Hungary). The average functionality of pMDI was ca. 2.8, while the content of free isocyanate groups was 31.5 %. Tin(II) 2-ethylhexanoate (Sn catalyst) produced by Sigma Aldrich, and tertiary amines Dabco® TMR-2 and Dabco® 1027 (Air Products Europe Chemicals BV) were used as catalysts. Tegostab® B 8465 (Evonik Industries AG) was employed as a stabilizer of porous structure. Carbon dioxide, generated in the reaction between water and isocyanate groups, was used as a chemical blowing agent. Solkane® 365/227 (Solvay Chemicals) served as a physical blowing agent.

Preparation of bio-based polyols

As mentioned before, bio-based polyols were synthesized by liquefaction of cellulose with purified crude glycerol. The mass ratio of solvent to biomass was 10:1. In order to accelerate the process, the catalyst (3 wt%) was added to the reaction mixture. The individual reactions were run at 120, 135 and 150 °C for 6 h, with samples being collected every hour. The obtained polyols were neutralized with a 67 % water solution of sodium hydroxide, and later dried out under vacuum.

Preparation of rigid polyurethane foams

Rigid polyurethane foams (PUFs) were produced on a laboratory scale by a single step method from a two-component (A and B) system with the ratio of NCO/OH groups equal to 2. Component A (polyol mixture) consisted of the estimated amount of polyether Rokopol RF 55 or a mixture of Rokopol RF55 and bio-based polyol at the appropriate ratio (prepared at 150 °C, as described in chapter 2.2), catalysts, surfactant and water. It was weighted and placed in a 500 mL polypropylene cup, then mixed with component B (polyisocyanate, pMDI) at a predetermined mass ratio, and stirred at 3000 rpm for 15 s, and left for free rise. After demoulding, the obtained PUF samples were kept at 60 °C for 24 h and then seasoned at room temperature for 24 h. Table 1 contains the details of different foam formulations.

Characterizations of polyols

The liquefaction extent was evaluated on the basis of the percentage of residue. The liquefaction product (1 g) was diluted (more than ten times) with methanol, then stirred by means of a magnetic stirrer for 4 h, and finally vacuum-filtered. Solid residue was washed with methanol and then dried in the oven at 100 °C until the sample has reached a constant weight. The percentage of residue was calculated according to formula (1):

$$m_{\text{residue}} = \frac{m}{m_o} \cdot 100 \quad (1)$$

where m (g) is the weight of residual biomass, and m_o (g) is the initial weight of biomass.

MOST WIEDZY Downloaded from mostwiedzy.pl

Table 1 The composition of reaction mixtures

Component	Foam's symbol				
	P1	P2	P3	P4	P5
	Mass of the component (g)				
Component A					
Rokopol RF55	11.15	8.55	7.25	5.95	3.55
Biopolyol EP1	–	2.60	3.90	5.30	7.80
DABCO 1027	0.165	0.165	0.165	0.165	0.165
DABCO TMR-2	0.165	0.165	0.165	0.165	0.165
Sn catalyst	0.06	0.06	0.06	0.06	0.06
TEGOSTAB B8465	0.15	0.15	0.15	0.15	0.15
Water	0.055	0.055	0.055	0.055	0.055
Solkane 365/227	5.0	5.0	5.0	5.0	5.0
Component B					
pMDI	21.02	23.75	25.12	26.49	29.22

The hydroxyl number of bio-based polyol was determined according to standard PN-93/C-89052/03. The samples weighing 0.5 g each were placed in 250 cm^3 Erlenmeyer flasks containing acetylating mixture and then heated for 30 min. Next, 1 mL of pyridine and 50 mL of distilled water were added. Finally, the resulting mixture was titrated using 0.5 M KOH solution in the presence of phenolphthalein indicator dye. The values of hydroxyl number were determined according to formula (2):

$$\mathrm{HV} = \frac{56.1 \cdot (V_2 - V_1) \cdot C_{\mathrm{KOH}}}{m} \quad (2)$$

where: C_{KOH}, concentration of KOH (mol/dm^3); V_1 and V_2, volumes of KOH used to titrate the analyzed sample (1) and blank (2), respectively (cm^3); and m, sample mass (g).

FT-IR spectrophotometric analysis was performed in order to determine the structure of the obtained bio-based polyol. The analysis was performed at a resolution of 4 cm^{-1} using a Nicolet 8700 apparatus (Thermo Electron Corporation) equipped with a snap-Gold State II which allowed for making the measurements in a reflection configuration mode.

The viscosity values of prepared polyols were determined using R/S Portable rheometer. The analysis was conducted at 25 °C for the shear rates varying from 1 to 100 s^{-1}. The obtained results were analyzed by employing Rheo 3000 computer software.

Oxidation Onset Temperature (OOT) Test. The OOT test was used to evaluate the effectiveness of antioxidants in biopolyols. The tests were performed under oxygen atmosphere using a NETSCH DSC F3 differential scanning calorimeter. The oxygen flow was maintained at 20 mL/min. The biopolyol samples (12 mg each) were placed in open aluminum pans and heated from 35 to 250 °C, at a heating rate of 10 °C/min. All the experiments were performed at least in duplicate. The OOT values were obtained by using the NETZSCH Proteus Thermal Analysis software.

The water content of the produced biopolyols was assessed by using Karl-Fischer titration. The samples were diluted with methanol and titrated with Fischer reagent.

The measurements of biopolyol density were performed at 25 °C by means of a pycnometer. The pH values were measured with a VOLTCRAFT pH-100 ATC pH-meter at 25 °C.

Characterization of polyurethanes

The apparent density of polyurethane samples was calculated in accordance with the standard PN–EN ISO 845: 2000 as the ratio of the sample weight to the sample volume. The volume of cube-shaped samples was measured with a slide caliper, with an accuracy of 0.1 mm. The samples were weighted using an electronic analytical balance, with an accuracy of 0.1 mg.

The compression strength of PUF samples was estimated in accordance with the standard PN–EN ISO 604:2006. The cube-shaped samples with the dimensions of 50 × 50 × 50 mm^3 were measured with a slide caliper, with an accuracy of 0.1 mm. The compression test was performed on a Zwick/Roell

MOST WIEDZY Downloaded from mostwiedzy.pl

tensile tester at a constant speed of 10 mm/min to 40 % deformation.

The thermogravimetric analysis (TGA) was performed on a NETZSCH TG 209 apparatus using 5-mg samples within the temperature range 100–600 °C under nitrogen atmosphere, at a heating rate of 15 °C/min.

The cellular morphology of polyurethanes was investigated with a Philips-FEI XL 30 environmental scanning electron microscope (ESEM) using an acceleration of 25 kV. Samples were cut at room temperature, while the observations were performed in wet mode.

Results and discussion

Characterization of bio-based polyols

As stated before, the liquefaction process was carried out at three different temperatures. In Fig. 1a, b, the values of biomass conversion and hydroxyl number plotted versus time and temperature of the process are presented. It is noticeable that an increase in reaction temperature resulted in the higher yield of liquefaction and lowered hydroxyl values in the obtained biopolyols.

Branched products prepared with applied crude glycerol were characterized by high hydroxyl values ranging between 650 and 1050 mg KOH/g. A noticeable drop in HV is related to the hydrolysis and alcoholysis reactions occurring during the biomass liquefaction. A decrease in the hydroxyl value with increasing reaction duration was also reported by others (Yao et al. 1995). The incorporation of high excess of glycerol may lead to its condensation and the resulting generation of polyglycerol and water as by-products. The balance between hydrolysis and alcoholysis shifts during the process, therefore the rate of hydroxyl value decrease is changing. Hydrolysis causes scission of biomass-derived long particles, leading to the generation of free hydroxyl groups, which are responsible for a momentary increase in HV. The degradation of biomass particles into low-molecular-weight compounds and their reactions with solvent present in the system reduces the content of residual biomass in the polyol. At the beginning of the process, such degradation is the primary process taking place, simultaneously causing a fast increase

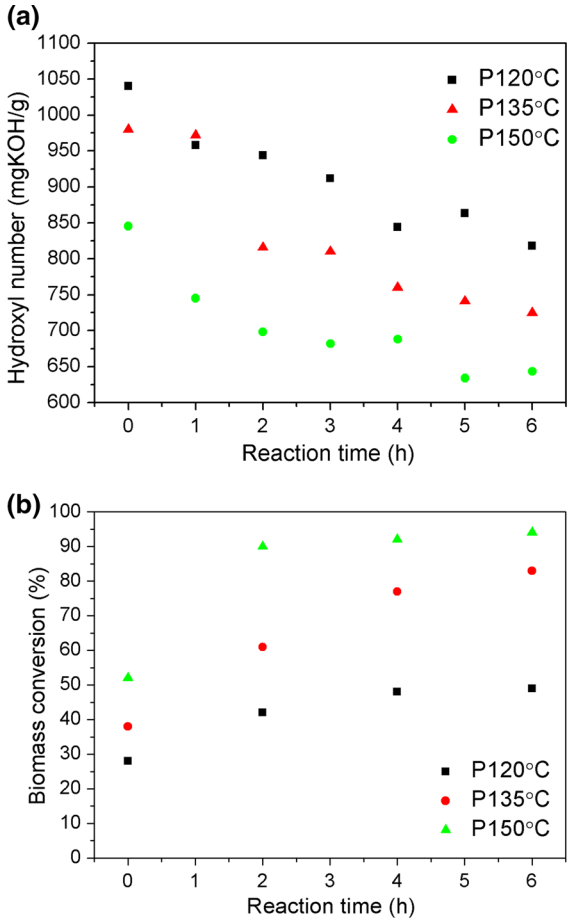

Fig. 1 Effect of reaction duration on the hydroxyl number (**a**) and yield of liquefaction (**b**) for different reaction temperatures

in the liquefaction yield. However, at the later stages of liquefaction, compounds generated through the biomass degradation are re-polymerizing, and thus creating an insoluble material that consists of glycol or glycerol glucosides and xylosides (Yamada and Ono 1999; Yamada et al. 2001). The re-polymerization rate increases with increasing reaction duration due to the increasing concentration of low-molecular-weight compounds related to the biomass decomposition (Wang and Chen 2007). As a result, the balance between decomposition and re-polymerization shifts towards the latter process, which simultaneously slows down the rate of increase of liquefaction yield. Undissolved residues of biomass present in the obtained polyol may act as reactive fillers during the polymer synthesis, e.g. they may react with isocyanates present in the reaction mixture during

MOST WIEDZY Downloaded from mostwiedzy.pl

polyurethane manufacturing. It can be seen that the values of hydroxyl number and liquefaction yield reach a plateau in about 5–6 h. Thus, on the basis of presented results, we can conclude that such reaction duration can be considered as optimal for lignocellulose biomass liquefaction process employing crude glycerol.

The measurements of rheological parameters enabled the determination of viscosity values, plotting of flow curves, and fitting the proper mathematical models to the obtained data.

In Fig. 2, the flow curves plotted for various reaction durations and temperatures are presented. The data demonstrate that the obtained biopolyols are non-Newtonian fluids because they display a nonlinear dependence of shear rate on shear stress (Chhabra 2010; Dziubiński et al. 2009). The slope of the initial part of flow curve is strictly correlated with the viscosity of the liquid, and can be described by the following formula (Schramm 2000) (3):

$$\tan\alpha = \eta_0 \tag{3}$$

In the presented plots, the slope value decreases with increasing reaction temperature, thus a decrease in viscosity has also occurred. Simultaneously, the maximum values of shear stress decreased, reaching 3290, 2302 and 1369 Pa at 120, 135 and 150 °C, respectively, for samples collected after a 6-h liquefaction.

The dependence of shear rate on the viscosity of biopolyols at various temperatures has been illustrated in Fig. 3. It is noticeable that after an initial increase, the viscosity decreases for higher values of shear rate. For the shear rates >ca. 80 s^{-1}, the relationship between the shear rate and viscosity becomes linear. Such disproportionality at low shear rates indicates that the prepared biopolyols should be categorized as pseudoplastic liquids (Björn et al. 2012). In such liquids, the increased shear rate results in a specific arrangement of particles, i.e. a steady flow arranges the particles along the flow line. At the beginning, the viscosity drop is quite rapid. Later on, when the particles reach the best possible arrangement, the viscosity decrease is slower. In the case of pseudoplastic liquids, decreasing viscosity due to increased shear rate is also the reason for describing these fluids as shear-thinning liquids (Glowiska and Datta 2014).

In Fig. 3, the values of viscosity measured at constant shear rate of 180 s^{-1} and constant temperature of 25 °C were plotted as a function of reaction temperature and reaction duration. It can be seen that with increasing reaction temperature and reaction duration there is a noticeable drop in viscosity, which correlates well with the estimated yield of

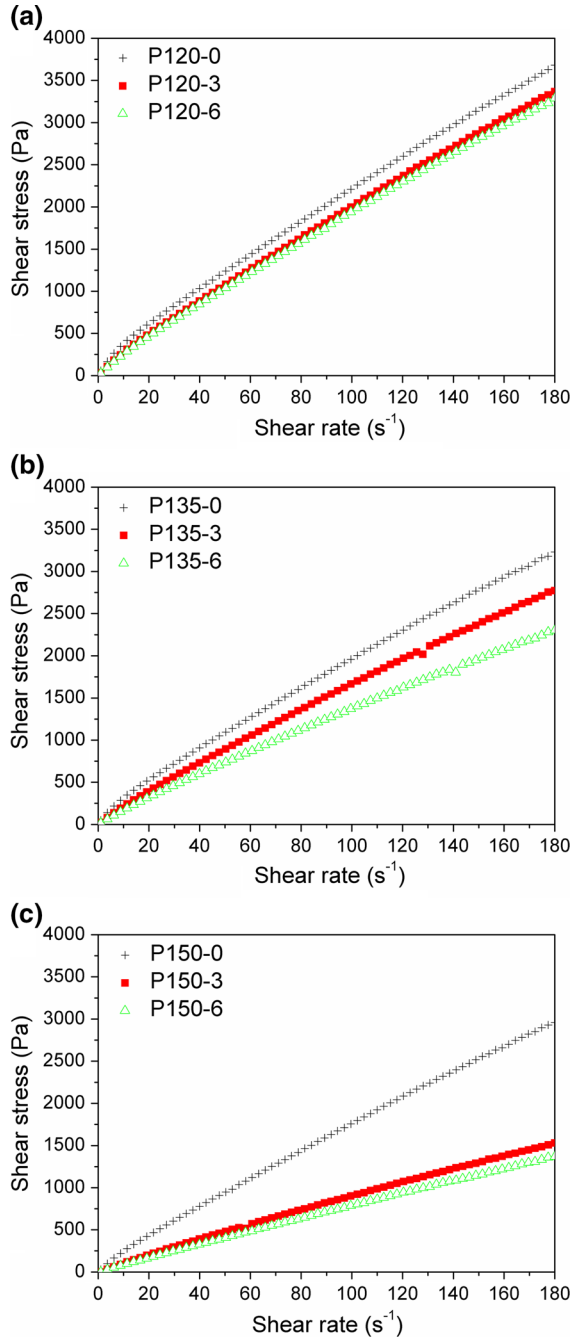

Fig. 2 Flow curves of biopolyols obtained at various temperatures: **a** 120 °C, **b** 135 °C, **c** 150 °C

MOST WIEDZY Downloaded from mostwiedzy.pl

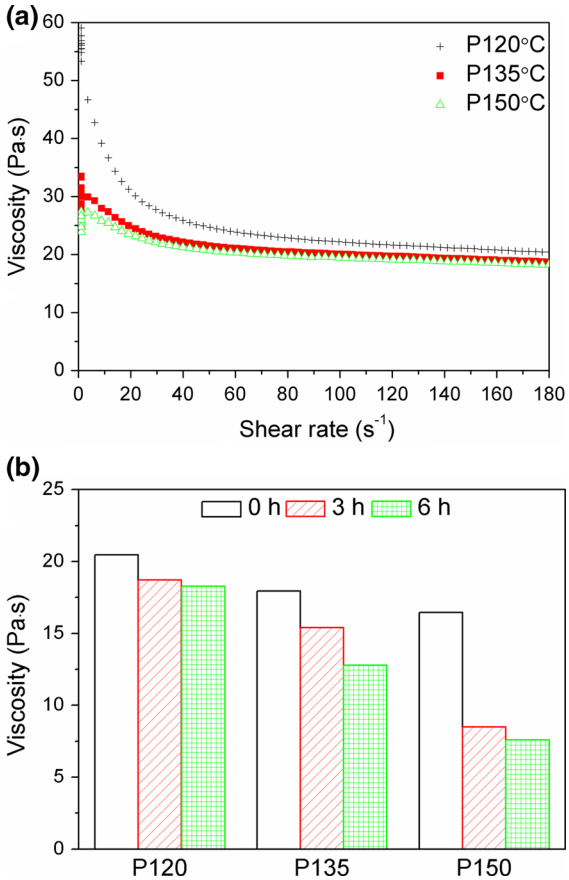

Fig. 3 The viscosity curves (**a**) and change in viscosity during the reaction (**b**)

liquefaction process. In Table 2, the mathematical models describing rheological behavior of the obtained polyols are presented. The rheological measurements were analyzed using the Ostwald-de Waele and Herschel Bulkley models. The Ostwald-de Waele model is a simple, but useful tool, employed to analyze the fluid behavior. However, the model only approximately describes the real non-Newtonian fluids. It is based on the following formulas (4) and (5):

$$\tau = K\left(\frac{\partial u}{\partial y}\right)^{n} \tag{4}$$

$$\mu_{\text{eff}} = K\left(\frac{\partial u}{\partial y}\right)^{n-1} \tag{5}$$

where K is the flow consistency index, $\partial u/\partial y$ is the shear rate perpendicular to the plane of shear, n is the flow behavior index, and μ_{eff} represents an effective viscosity as a function of shear rate.

The presented formulas implicate that for liquids with value of n lower than 1, effective viscosity would drop indefinitely with increasing shear rate. Thus the Ostwald-de Waele model is suitable for analyzing fluids within a given range of shear rates. Based on the flow behavior index n, fluids can be divided into three categories, i.e. pseudoplastic (n lower than 1), Newtonian (n equals 1) and dilatant (n higher than 1) fluids. The value of index n lower than 1 for all prepared biopolyols confirms the assumption made on the basis of flow curves, namely, that the obtained liquids can be classified as pseudoplastic. Moreover, the increased time of reaction duration caused an increase in the flow behavior index. This means that longer reaction duration shifts the fluid behavior closer to Newtonian fluids.

Herschel-Bulkley model is based on the following constitutive Eq. (6):

$$\tau = \tau_0 + K\dot{\gamma}^{n} \tag{6}$$

where τ is the shear stress, τ_0 yield stress, $\dot{\gamma}$ shear rate, K is the flow consistency index, and n the flow behavior index.

Yield stress is a very important parameter of the Herschel-Bulkley model as it determines the amount of stress that fluid may experience before it starts to flow. With increasing reaction duration and temperature, the value of yield stress becomes significantly reduced, which is strictly related to the yield of liquefaction and the percentage of solid residue in a biopolyol. The presence of solid particles in the fluid increases the force needed to make fluid flow. Thus, the degradation of lignocellulose-biomass particles during liquefaction resulted in a decrease in yield stress, which equaled zero after a 6-h reaction. This indicates that the biopolyols were flowing immediately after the application of force.

As in the case of the Ostwald-de Waele model, the n value determines the shear thinning or shear thickening of the fluid, for example, for $n = 1$ and $\tau_0 = 0$, the model describes fluid as Newtonian. According to the Herschel-Bulkley model, the prepared biopolyols are pseudoplastic fluids, which is in agreement with the flow curves and the Ostwald-de Waele model developed for the tested polyols.

Figure 4 shows FTIR spectra for biopolyol obtained at 150 °C, after 6 h of reaction, together with the spectra of substrates used, glycerol and cellulose. Absorption bands (a) characteristic for the

MOST WIEDZY Downloaded from mostwiedzy.pl

Table 2 The Ostwald-de Waele and Herschel Bulkley linear functions based on the rheological data from bio-based polyol samples

Sample code	Function	K (Pa s^n)	n (−)	R^2
The Ostwald-de Waele linear functions				
P120-0	$y = 56.46\ x^{0.7984}$	56.4605	0.7984	0.9995
P120-3	$y = 31.51\ x^{0.9031}$	31.5098	0.9031	0.9999
P120-6	$y = 26.97\ x^{0.9305}$	26.9727	0.9305	0.9996
P135-0	$y = 45.31\ x^{0.8194}$	45.3099	0.8194	0.9999
P135-3	$y = 22.78\ x^{0.9331}$	22.7751	0.9331	0.9993
P135-6	$y = 17.38\ x^{0.9501}$	17.3832	0.9501	0.9990
P150-0	$y = 28.33\ x^{0.8982}$	28.3265	0.8982	0.9999
P150-3	$y = 11.76\ x^{0.9424}$	11.7573	0.9424	0.9997
P150-6	$y = 9.42\ x^{0.9611}$	9.4196	0.9611	0.9999

Sample code	Function	τ_0 (Pa)	μ_{om} (Pa s^n)	n (−)	R^2
The Herschel Bulkley linear functions					
P120-0	$y = 33.02 + 41.64\ x^{0.8605}$	33.02	41.6439	0.8605	0.9998
P120-3	$y = 2.76 + 33.23\ x^{0.8899}$	2.76	33.2346	0.8899	0.9999
P120-6	$y = 30.94\ x^{0.8987}$	0	30.9436	0.8987	0.9999
P135-0	$y = 15.33 + 38.71\ x^{0.8513}$	15.33	38.7101	0.8513	0.9999
P135-3	$y = 28.25\ x^{0.8848}$	0	28.2459	0.8848	0.9999
P135-6	$y = 22.70\ x^{0.89}$	0	22.7013	0.8900	0.9999
P150-0	$y = 4.71 + 28.96\ x^{0.8911}$	4.71	28.9640	0.8911	0.9999
P150-3	$y = 13.78\ x^{0.9073}$	0	13.7771	0.9073	0.9998
P150-6	$y = 10.08\ x^{0.9459}$	0	10.0808	0.9459	0.9999

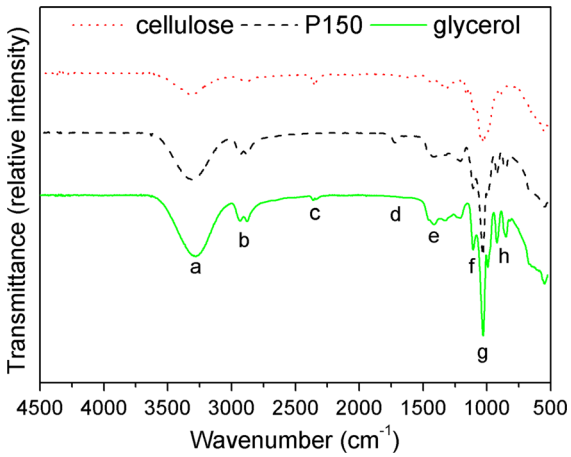

Fig. 4 FTIR spectra of cellulose, glycerol and bio-based polyol

stretching vibrations of O–H groups were observed at 3300 cm^{-1} (Deng and Ting 2005). Signals (b) in the range of 2940–2870 cm^{-1} were attributed to the symmetric and asymmetric stretching vibrations of C–H bonds in CH_2 groups present in aliphatic chains and CH_3 end groups (Collier et al. 1997). The absorption maxima (c) at ca. 2360–2320 cm^{-1} were most likely associated with the weak vibrations of acetal groups present in the cellulose structure. A band (d) at 1720 cm^{-1} was attributed to the stretching vibrations of unconjugated C=O bonds and C=C bonds in the products of cellulose degradation that had occurred during the liquefaction of biomass (Budarin et al. 2010). Signals (e) in the range between 1420 and 1333 cm^{-1} were related to the CH_2 and HOC in-plane bending vibrations (Ciolacu et al. 2011; Schwanninger et al. 2004). The absorption bands observed between 1170 and 980 cm^{-1} (g) were characteristic for the vibrations of C–O–C ether groups (Cai et al. 2007). Other signals (h) observed at 915–840 cm^{-1} can be attributed to the out-of-plane vibrations of C=C and C–H bonds in aromatic rings present in the structure of biomass used (Faix 1991).

In the present study, FTIR analysis was used for qualitative purposes. Nevertheless, some dependences in the intensity of particular signals might be observed. In case of biopolyol spectra is quite similar to those of

MOST WIEDZY Downloaded from mostwiedzy.pl

applied glycerol, which is related to the excess of this solvent used during liquefaction.

In Table 4, the values of density, water content and pH of the obtained biopolyols are presented. It can be seen that the reaction temperature does not have a significant influence on the density and pH of the produced materials. All samples had density of 2.7 g/cm^3, while their pH ranged from 6.5 to 6.7. The water content of liquefied cellulose and crude glycerol was 5.4 and 0.5 wt%, respectively. Considering these values and the fact that water was present in the catalyst and KOH solution used for neutralization, the theoretical water content of the obtained polyols should have been ca. 0.97 wt%. Prior to desiccation, the water content was 2.1, 4.3 and 12.4 wt% for the polyols obtained at 120, 135 and 150 °C, respectively. This finding demonstrates that water is generated as a by-product during the biomass liquefaction (Wang et al. 2009a, b). Nevertheless, the final water content decreased with increasing reaction temperature, which means that higher temperature reduces the amount of bonded water in the forming polyols.

The values of OOT were determined for the samples coded P120, P135 and P150 after 6 h of reaction (see Table 3). The oxidation onset temperature was defined as the intersection of the tangent line to the initial baseline and the tangent line to the point of maximum increase, corresponding to the inflection point of the oxidation peak.

The presented data indicate that the increased temperature of liquefaction enhances oxidative stability of resulting biopolyols. Such phenomenon can be associated with the specifics of the process. As mentioned before, during liquefaction cellulose is decomposing into low-molecular-weight compounds with various functional groups, which can be subjected to oxidation, e.g. hydroxyl groups. These compounds are subsequently reacting with the solvent, which decreases the hydroxyl value of biopolyols. As illustrated in Fig. 1, the hydroxyl value and percentage of solid residue decrease with increasing temperature, so there are less functional groups prone to oxidation. This means that an increase in the liquefaction yield will result in the higher value of OOT.

The results of thermogravimetric analysis of raw materials and biopolyols obtained after a 6-h reaction are presented in Fig. 5 and Table 4. As can be observed on the DTG curve, raw materials displayed rather sharp peaks which is related to the level of material's purity. In the case of cellulose, a small degradation step at ca. 100 °C is related to the moisture content of the material, while the further course of degradation is typical for this compound (Shafizadeh and Bradbury 1979; Shen and Gu 2009). Thermal stability of the prepared biopolyols increased

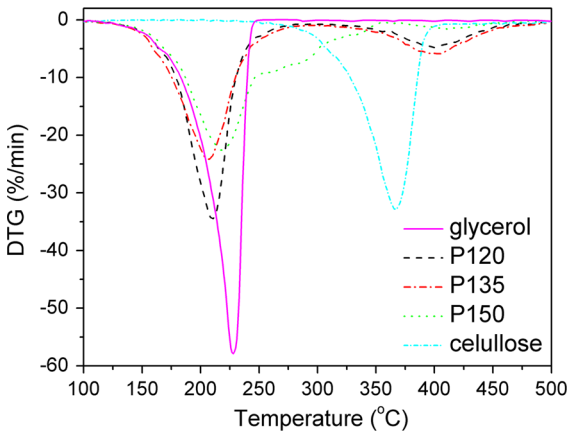

Fig. 5 Differential thermogravimetric curves for cellulose, glycerol and bio-based polyol after a 6-h reaction

Table 3 Physical properties of bio-based polyol obtained after 6 h of reaction

Property	Sample		
	P120	P135	P150
Density (g/cm)	2.7	2.7	2.7
Water content before drying (%)	2.1	4.3	12.4
Water content after drying (%)	1.34	0.95	0.63
pH value	6.5	6.7	6.7
OOT (°C)	161	175	180

Table 4 Thermogravimetric analysis of bio-based polyol, cellulose and glycerol

Sample	Temperature (°C)				
	T_2	T_5	T_{10}	$T_{max\ 1}$	$T_{max\ 2}$
P120	144	163	176	206	404
P135	152	168	181	210	401
P150	153	173	188	220	413
Cellulose	63	272	313	–	369
Glycerol	148	167	182	228	–

MOST WIEDZY Downloaded from mostwiedzy.pl

with increasing reaction temperature, as these two parameters are strongly correlated. As in the case of OOT, a higher reaction temperature resulted in the lowered content of compounds with weak thermal stability in the analyzed biopolyols because the latter had been subjected to various chemical reactions during liquefaction.

In addition, noticeable differences in DTG curves of the analyzed polyols are present, which can be related to the effectiveness of liquefaction process. The values of $T_{max\ 1}$ and $T_{max\ 2}$ are shifted towards higher temperatures, which is related to the higher yield of liquefaction and more effective bonding of liquefied cellulose to the solvent particles. In the case of sample P150, both temperature peaks are lowered, while its thermal degradation within the range of 250–350 °C differs compared to other samples. These findings indicate a better material homogeneity and the compatibility between the compounds present in this particular biopolyol.

Mechanical and thermal properties of analyzed polyurethanes

In Table 5, the values of apparent density and compressive strength of prepared rigid polyurethane foams are presented.

In the case of polyurethane foams, apparent density has a crucial impact on the mechanical performance of the material due to the fact that higher density results in the increased compressive strength (Prociak 2008). The replacement of petrochemical polyol with biopolyol P150 resulted in a decreased volumetric expansion during polymerization which, in turn, caused an increase in the produced material's density in comparison to neat foam. Similar observations associated with the incorporation of bio-based polyols into polyurethane foams have been previously reported (Piszczyk et al. 2014). However, the effect related to the use of P150 is rather small due to the low water content of the biopolyol used in this study in comparison to biopolyols described in the literature. An increased share of biopolyol in the polyol mixture improved the mechanical strength of the obtained material, which can be related to the slight increase in apparent density. Nevertheless, the highest value of compressive strength was observed for sample P3, which indicates a synergistic effect between the applied polyols.

The incorporation of bio-based polyol into PU foam also increased the average cell size, as illustrated in Fig. 6. Such phenomenon might be related to the higher water content of biopolyol P150 (0.63 wt%) compared to Rokopol RF55 (<0.1 wt%), and a slightly higher generation of carbon dioxide during the reaction with isocyanate particles present in the system. The decreased viscosity of polyol mixture might be another underlying reason since P150 has lower viscosity than the petrochemical polyol (7600 and 9200 mPa s, respectively) which facilitates the diffusion of CO_2 and hydrofluorocarbon used. Similar results related to the increase of cell size during the incorporation of bio-based polyols into polyurethane foams have been reported by others (Zieleniewska et al. 2015).

The results of thermogravimetric analysis are presented in Fig. 7 and Table 6. Generally, the mechanism of polyurethane thermal degradation is rather complicated due to the complex structure of the material. For all samples, the values of the initial temperature of degradation corresponding to 2 and 5 wt% mass loss were in the range of 188–259 °C, which is related to the initial stage of polyurethane degradation, involving the decomposition of less stable groups such as, biuret, alophanate and urethane (Lee et al. 2002; Somania et al. 2003; Tanaka et al. 2008). The consecutive steps of degradation consisted of the decomposition of long polyol chains, and were relatively slower than the first step (Cervantes-Uc et al. 2009).

Table 5 Comparison of the properties of rigid polyurethane foams

Sample	Apparent density (kg/m^3)	Cell size (μm)	Compressive strength (kPa)
P1	39.3 ± 1.6	129.8 ± 6.5	267.0 ± 7.3
P2	39.6 ± 1.9	152.7 ± 7.6	256.5 ± 6.5
P3	40.3 ± 1.3	180.7 ± 7.0	320.0 ± 6.8
P4	41.7 ± 1.5	189.5 ± 6.8	352.6 ± 7.8
P5	42.5 ± 1.8	202.2 ± 7.2	367.4 ± 7.0

MOST WIEDZY Downloaded from mostwiedzy.pl

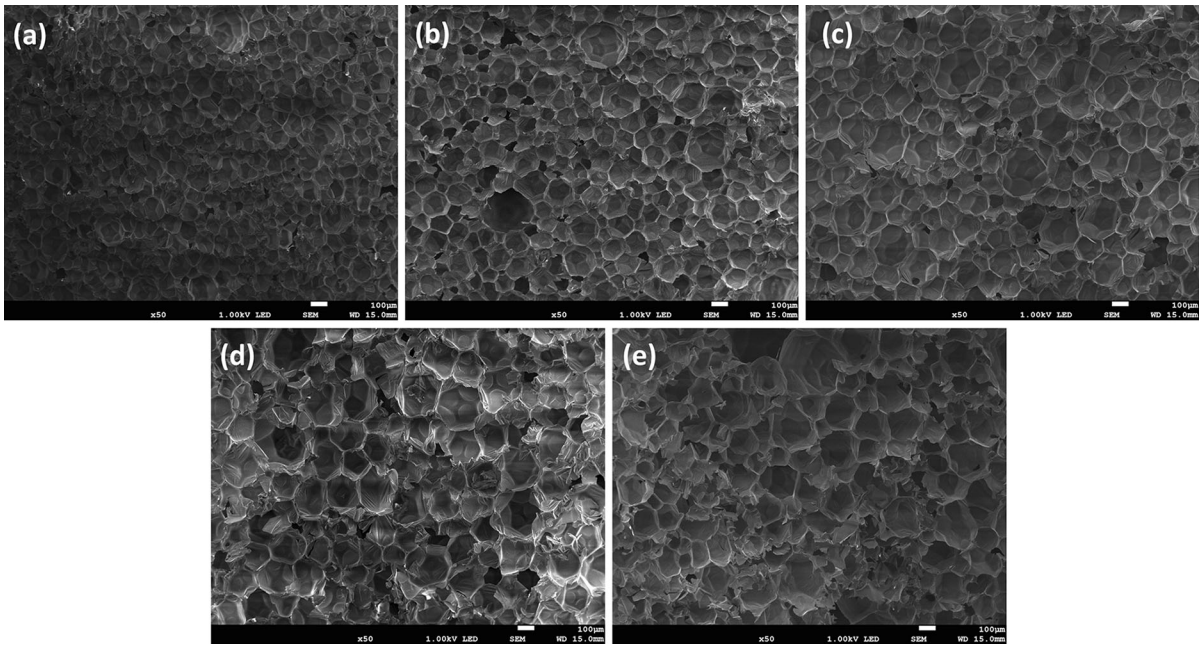

Fig. 6 SEM images of PU foams coded **a** P1, **b** P2, **c** P3, **d** P4 and **e** P5

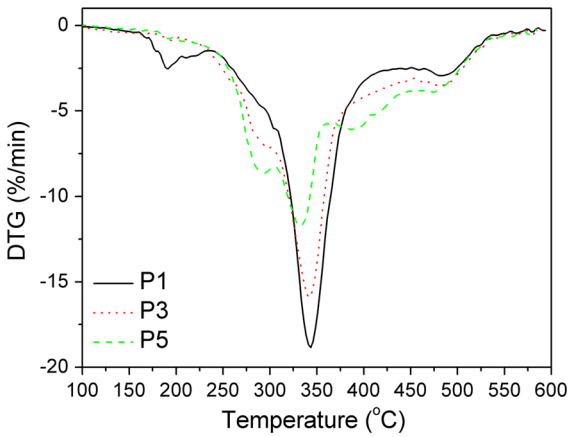

Fig. 7 The effect of bio-based polyol on the shape of differential thermogravimetric curves for rigid polyurethane foams

It is noticeable that the incorporation of P150 biopolyol resulted in the increased thermal stability of PU foam, which may suggest a decrease in the content of volatile compounds and the enhancement of thermal stability of rigid segments in the resulting material. In Table 6, the values of $T_{max\ 1}$, $T_{max\ 2}$, $T_{max\ 3}$ and $T_{max\ 4}$, respectively corresponding to the temperature peaks on the differential thermogravimetric curves are presented. Moreover, the DTG curves are presented in Fig. 7 in order to illustrate the slight changes in thermal degradation pathways of the analyzed foams. It can be seen that the incorporation of biopolyol residues into rigid polyurethane foams caused the disappearance of $T_{max\ 1}$ peak that has been "replaced" by $T_{max\ 2}$ peak. This confirms the delay of thermal degradation of rigid segments. The $T_{max\ 3}$ peak, which is related to the

Table 6 Characteristics of thermal degradation in rigid polyurethane foams

Sample	Mass loss (wt%)				$T_{max\ 1}$ (°C)	$T_{max\ 2}$ (°C)	$T_{max\ 3}$ (°C)	$T_{max\ 4}$ (°C)
	2	5	10	50				
	Temperature (°C)							
P1	188	217	269	354	190	–	343	483
P3	199	249	277	366	–	297	342	481
P5	215	259	282	377	–	298	335	478

MOST WIEDZY Downloaded from mostwiedzy.pl

decomposition of soft segments, shifted towards lower temperatures with the increasing content of biopolyol. This finding suggests a slight deterioration of soft segment stability. For all the analyzed foams, peak $T_{max\ 4}$ was present which is associated with the thermolysis of organic residues from previous decomposition stages (Garrido and Font 2015).

Conclusions

Biopolyols suitable for the manufacturing of rigid polyurethane foams were prepared via lignocellulose-biomass liquefaction process, with the refined crude glycerol used as a solvent. To better control the mechanism of the process, pure cellulose was used as a raw material. The effect of liquefaction time and temperature on the effectiveness of the process, and the parameters of the resulting biopolyols were characterized. The produced materials were analyzed in terms of their structure (FTIR analysis), water content, hydroxyl value, and rheological (viscosity studies) and thermal (thermogravimetric analysis, oxidation onset temperature test) properties. The reaction duration of 6 h and a temperature of 150 °C were selected as optimal parameters for the production of biopolyol to be used later for obtaining rigid polyurethane foams. The foam sample P150, obtained in the reaction with a 94 % yield, was characterized by the hydroxyl number of 643 mg KOH/g. Moreover, with increasing reaction temperature the thermal stability and resistance to oxidation of the polyol improved, which was strictly correlated to the mechanism of the liquefaction process.

The obtained biopolyols were also analyzed with respect to their rheological properties. The produced materials showed the viscosity values similar to those of commercially available products commonly used for manufacturing of PU foams. This finding should be considered as very beneficial from the technological point of view. The obtained rheological data were analyzed using the Ostwald-de Waele and Herschel Bulkley models. According to these mathematical models, the prepared biopolyols can be classified as pseudoplastic fluids. However, with increasing reaction duration the character of polyols is closer to a Newtonian fluid.

Biopolyol P150 was selected for the preparation of rigid polyurethane foams; its share in the polyol mixture was variably increased to 70 wt%. The obtained foams were characterized in terms of their basic properties such as, apparent density, cell size, compressive strength, and thermal stability. The presented results indicate that the substitution of petrochemical polyol with the obtained bio-based polyol slightly increased the apparent density of the material. However, the differences were small and they could be easily corrected by adjusting the foam formulation (i.e. foaming agent content). Moreover, the incorporation of biopolyol resulted in the increased average cell size, but this change in the foam morphology did not have any unfavorable influence on the mechanical performance of the material. The highest value of compressive strength was observed for sample P3 (35 wt% of biopolyol in the polyol mixture), which indicates a synergistic effect between the applied polyols. The analyzed modifications with polyol P150 also enhanced the thermal stability of PU foams, as demonstrated by a slight change in the thermal decomposition process.

In summary, this work has confirmed that lignocellulose-biomass liquefaction with refined crude glycerol can be successfully applied to manufacture polyols used in the polyurethane foam production. The resulting polyols allowed the preparation of foams with comparable or even enhanced properties compared to the foams produced with petrochemical compounds only. Further studies in this field should focus on (1) the evaluation of crude glycerol containing impurities as a solvent for the biomass liquefaction process; (2) the application of other, more complex types of biomass, including the biomass of industrial origin; (3) the investigation of total substitution of petrochemical polyols with those obtained via lignocellulose-biomass liquefaction for the production of polyurethane foams.

Open Access This article is distributed under the terms of the Creative Commons Attribution 4.0 International License (http://creativecommons.org/licenses/by/4.0/), which permits unrestricted use, distribution, and reproduction in any medium, provided you give appropriate credit to the original author(s) and the source, provide a link to the Creative Commons license, and indicate if changes were made.

MOST WIEDZY Downloaded from mostwiedzy.pl

References

Arbenz A, Averous L (2015) Oxyalkylation of gambier tannin—synthesis and characterization of ensuing biobased polyols. Ind Crop Prod 67:295–304. doi:10.1016/j.indcrop.2015.01.073

Baek IG, You SJ, Park ED (2012) Direct conversion of cellulose into polyols over Ni/W/SiO_2-Al_2O_3. Bioresour Technol 114:684–690. doi:10.1016/j.biortech.2012.03.059

Björn A, Segura de La Monja P, Karlsson A, Ejlertsson J, Svensson BH (2012) In: Kumar S (ed) Rheological characterization. Biogas. InTech publisher, Rijeka

Briones R, Serrano L, Melus A, Herseczki Z, Labidi J (2010) Polyols from the lignocellulosic waste of biodiesel production process. Chem Eng Trans 21:1339–1344. doi:10.3303/CET1021224

Briones R, Serrano L, Llano-Ponte R, Labidi J (2011a) Polyols obtained from solvolysis liquefaction of biodiesel production solid residues. Chem Eng J 175:169–175. doi:10.1016/j.cej.2011.09.090

Briones R, Serrano L, Younes RB, Mondragon I, Labidi J (2011b) Polyol production by chemical modification of date seeds. Ind Crop Prod 34:1035–1040. doi:10.1016/j.indcrop.2011.03.012

Budarin VL, Clark JH, Lanigan BA, Shuttleworth P, Macquarrie DJ (2010) Microwave assisted decomposition of cellulose: a new thermochemical route for biomass exploitation. Bioresour Technol 101:3776–3779. doi:10.1016/j.biortech.2009.12.110

Cai Z, Gao J, Li X, Xiang B (2007) Synthesis and characterization of symmetrical benzodifuranone compounds with femtosecond time-resolved degenerate four-wave mixing technique. Opt Commun 272:503–508. doi:10.1016/j.optcom.2006.11.056

Cervantes-Uc JM, Moo Espinosa JI, Cauich-Rodriguez JV, Avila-Ortega A, Vazquez-Torres H, Marcos-Fernandez A, San Roman J (2009) TGA/FTIR studies of segmented aliphatic polyurethanes and their nanocomposites prepared with commercial montmorillonites. Polym Degrad Stab 94:1666–1677. doi:10.1016/j.polymdegradstab.2009.06.022

Chhabra RP (2010) Non-Newtonian fluids: an introduction. In: Deshpande AP, Krishnan JM, Kumar S (eds) Rheology of complex fluids. Springer, Berlin, pp 3–34. doi:10.1007/987-1-4419-6494-6_1

Cinelli P, Anguillesi I, Lazzeri A (2013) Green synthesis of flexible polyurethane foams from liquefied lignin. Eur Polym J 49:1174–1184. doi:10.1016/j.eurpolymj.2013.04.005

Ciolacu D, Ciolacu F, Popa V (2011) Amorphous cellulose—structure and characterization. Cell Chem Technol 45:13–21

Collier W, Kalasinsky VF, Schultz TP (1997) Infrared study of lignin: reexamination of Aryl-Alkyl Ether C–O stretching peak assignments. Holzforschung 51:167–168. doi:10.1515/hfsg.1992.46.6.523

Deng S, Ting YP (2005) Characterization of PEI-modified biomass and biosorption of Cu(II), Pb(II) and Ni, (II). Water Res 39:2167–2177. doi:10.1016/j.watres.2005.03.033

Dziubinski M, Kiljanski T, Sek J (2009) Podstawy reologii i reometrii płynów. Lodz Unversity of Technology Publisher, Lodz

Evtiouguina M, Barros A, Pinto JC, Neto CP, Belgacem MN, Gandini A (2002) Oxypropylation of cork and the use of the ensuing polyols in polyurethane for mulations. Biomacromolecules 3:57–62. doi:10.1021/bm010100c

Faix O (1991) Classification of lignins from different botanical origins by FT-IR spectroscopy. Holzforschung 45:21–27. doi:10.1515/hfsg.1991.45.s1.21

Garrido MA, Font R (2015) Pyrolysis and combustion study of flexible polyurethane foam. J Anal Appl Pyrol 113:202–215. doi:10.1016/j.jaap.2014.12.017

Głowiska E, Datta J (2014) A mathematical model of rheological behawior of novel bio-based isocyanate-terminated polyurethane prepolymers. Ind Crop Prod 60:123–129. doi:10.1016/j.indcrop.2014.06.016

Hassan EM, Shukry N (2008) Polyhydric alcohol liquefaction of some lignocellulosic agricultural residues. Ind Crop Prod 27:33–38. doi:10.1016/j.indcrop.2007.07.004

Hu S, Li Y (2014) Two-step sequential liquefaction of lignocellulosic biomass by crude glycerol for the production of polyols and polyurethane foams. Bioresour Technol 161:410–415. doi:10.1016/j.biortech.2014.03.072

Hu S, Wan C, Li Y (2012) Production and characterization of biopolyols and polyurethane foams from crude glycerol based liquefaction of soybean straw. Bioresour Technol 103:227–233. doi:10.1016/j.biortech.2011.09.125

Jin Y, Ruan X, Cheng X, Lu Q (2011) Liquefaction of lignin by polyethyleneglycol and glycerol. Bioresour Technol 102:3581–3583. doi:10.1016/j.biortech.2010.10.050

Kurimoto Y, Koizumi A, Doi S, Tamura Y, Ono H (2001) Wood species effects in the characteristics of liquefied wood and properties of polyurethane films prepared from the liquefied wood. Biomass Bioenerg 21:381–390. doi:10.1016/S0961-9534(01)00041-1

Lee SH, Teramoto Y, Shiraishi N (2002) Biodegradable polyurethane foam from liquefied waste paper and its thermal stability, biodegradability, and genotoxicity. J Appl Polym Sci 83:1482–1489. doi:10.1002/app.10039

Liu M, Wang H, Han J, Niu Y (2012) Enhanced hydrogenolysis conversion of cellulose to C2–C3 polyols via alkaline pretreatment. Carbohydr Polym 89:607–612. doi:10.1016/j.carbpol.2012.03.058

Mahmood N, Yuan Z, Schmidt J, Xu C (2013) Production of polyols via direct hydrolysis of kraft lignin: effect of process parameters. Bioresour Technol 130:13–20. doi:10.1016/j.biortech.2013.03.199

Maki-Arvela P, Anugwom I, Virtanen P, Sjoholm R, Mikkola JP (2010) Dissolution of lignocellulosic materials and its constituents using ionic liquids—a review. Ind Crop Prod 32:175–201. doi:10.1016/j.indcrop.2010.04.005

Matos M, Barreiro MF, Gandini A (2010) Olive stone as a renewable source of biopolyols. Ind Crop Prod 32:7–12. doi:10.1016/j.indcrop.2010.02.010

Matsunaga M, Matsui H, Otsuka Y, Yamamoto S (2008) Chemical conversion of wood by treatment in a semi-batch reactor with subcritical water. J Supercrit Fluid 44:364–369. doi:10.1016/j.supflu.2007.09.011

MOST WIEDZY Downloaded from mostwiedzy.pl

Miller JE, Evans L, Littlewolf A, Trudell DE (1999) Batch microreactor studies of lignin and lignin model compound depolymeryzation by bases in alcohol solvents. Fuel 78:1363–1366. doi:10.1016/S0016-2361(99)00072-1

Minami E, Saka S (2003) A comparative study of decomposition behaviors between hardwood and softwood in supercritical methanol. J Wood Sci 49:73–78. doi:10.1007/s100860300012

Pavier C, Gandini A (2000) Oxypropylation of sugar beet pulp. 1. Optimisation of the reaction. Ind Crop Prod 12:1–8. doi:10.1016/S0926-6690(99)00039-4

Piszczyk Ł, Strankowski M, Danowska M, Hejna A (2014) Rigid polyurethane foams from a polyglycerol-based polyol. Eur Polym J 57:143–150. doi:10.1016/j.eurpolymj.2014.05.012

Poudel J, Oh SC (2012) Degradation characteristics of wood using supercritical alcohols. Energies 5:5038–5052. doi:10.3390/en5125038

Prociak A (2008) Właściwości termoizolacyjne sztywnych pianek poliuretanowych syntetyzowanych z udziałem polioli z olejów roślinnych. Polimery 53:195–200

Rosa JR, Silva ISV, Lima CSM, Pasquini D (2015) Production of polyols and new biphasic mono-component materials from soy hulls by oxypropylation. Ind Crop Prod 72:152–158. doi:10.1016/j.indcrop.2014.12.044

Roslan R, Zakaria S, Chia CH, Boehm R, Laborie MP (2014) Physico-mechanical properties of resol phenolic adhesives derived from liquefaction of oil palm empty fruit bunch fibres. Ind Crop Prod 62:119–124. doi:10.1016/j.indcrop.2014.08.024

Schramm G (2000) A practical approach to rheology and rheometry, 2nd edn. Gebrueder HAAKE GmbH, Karlsruhe, pp 18–19

Schwanninger M, Rodrigues JC, Pereira H, Hinterstoisser B (2004) Effects of short-time vibratory ball milling on the shape of FT-IR spectra of wood and cellulose. Vib Spectrosc 36:23–40. doi:10.1016/j.vibspec.2004.02.003

Shafizadeh F, Bradbury AGW (1979) Thermal degradation of cellulose in air and nitrogen at low temperatures. J Appl Polym Sci 23:1431–1442. doi:10.1002/app.1979.070230513

Shen DK, Gu S (2009) The mechanism for thermal decomposition of cellulose and its main products. Bioresour Technol 100:6496–6504. doi:10.1016/j.biortech.2009.06.095

Somania KP, Kansaraa SS, Patelb NK, Rakshit AK (2003) Castor oil based polyurethane adhesives for wood-to-wood bonding. Int J Adhes Adhes 23:269–275. doi:10.1016/S0143-7496(03)00044-7

Tanaka R, Hirose S, Hatakeyama H (2008) Preparation and characterization of polyurethane foams using a palm oil-based polyol. Bioresour Technol 99:3810–3816. doi:10.1016/j.biortech.2007.07.007

Wang H, Chen HZ (2007) A novel method of utilizing the biomass resource: rapid liquefaction of wheat straw and preparation of biodegradable polyurethane foam (PUF). J Chin Inst Chem Eng 38:95–102. doi:10.1016/j.jcice.2006.10.004

Wang T, Zhang L, Li D, Yin J, Wu S, Mao Z (2008) Mechanical properties of polyurethane foams prepared from liquefied corn stover with PAPI. Bioresour Technol 99:2265–2268. doi:10.1016/j.biortech.2007.05.003

Wang M, Xu CC, Leitch M (2009a) Liquefaction of cornstalk in hot-compressed phenol-water medium to phenolic feedstock for the synthesis of phenol-formaldehyde resin. Bioresour Technol 100:2305–2307. doi:10.1016/j.biortech.2008.10.043

Wang Y, Wu J, Wan Y, Lei H, Yu F, Chen P, Lin X, Liu Y, Ruan R (2009b) Liquefaction of corn stover using industrial biodiesel glicerol. Int J Agr Biol Eng 2(2):32–40. doi:10.3965/j.issn.l934-6344.2009.02.032-040

Yamada T, Ono H (1999) Rapid liquefaction of lignocellulosic waste by using ethylene carbonate. Bioresour Technol 70:61–67. doi:10.1016/S0960-8524(99)00008-5

Yamada T, Hu YH, Ono H (2001) Condensation reaction of degraded lignocellulose during wood liquefaction in the presence of polyhydric alcohols. Nippon Setchaku Gakkaishi 37:471–478. doi:10.11618/adhesion.37.471

Yao Y, Yoshioka M, Shiraishi N (1995) Rigid polyurethane foams from combined liquefaction mixtures of wood and starch. Mokuzai Gakkaishi 41:659–668

Ye L, Zhang J, Zhao J, Tu S (2014) Liquefaction of bamboo shoot shell for the production of polyols. Bioresour Technol 153:147–153. doi:10.1016/j.biortech.2013.11.070

Yona AMC, Budija F, Kricel B, Kutnar A, Pavlic Tavzes C, Petric M (2014) Production of biomaterials from cork: liquefaction on polyhydric alcohols at moderate temperatures. Ind Crop Prod 54:296–301. doi:10.1016/j.indcrop.2014.01.027

Zhang T, Zhou Y, Liu D, Petrus L (2007) Qualitative analysis of products formed during the acid catalyzed liquefaction of bagasse in ethylene glycol. Bioresour Technol 98:1454–1459. doi:10.1016/j.biortech.2006.03.029

Zhang H, Ding F, Luo C, Xiong L, Chen X (2012) Liquefaction and characterization of acid hydrolysis residue of corncob in polyhydric alcohols. Ind Crop Prod 39:47–51. doi:10.1016/j.indcrop.2012.02.010

Zhang H, Yang H, Guo H, Huang C, Xiong L, Chen X (2014) Kinetic study on the liquefaction of wood and its three cell wall component in polyhydric alcohols. Appl Energ 113:1596–1600. doi:10.1016/j.apenergy.2013.09.009

Zieleniewska M, Leszczyński MK, Kurańska M, Prociak A, Szczepkowski L, Krzyżowska M, Ryszkowska J (2015) Preparation and characterisation of rigid polyurethane foams using arapeseed oil-based polyol. Ind Crop Prod 74:887–897. doi:10.1016/j.indcrop.2015.05.081

MOST WIEDZY Downloaded from mostwiedzy.pl